

REPORT DOCUMENTATION PAGE

*Form Approved
OMB No. 0704-0188*

Public reporting burden for this collection of information is estimated to average 1 hour per response, including the time for reviewing instructions, searching existing data sources, gathering and maintaining the data needed, and completing and reviewing this collection of information. Send comments regarding this burden estimate or any other aspect of this collection of information, including suggestions for reducing this burden to Department of Defense, Washington Headquarters Services, Directorate for Information Operations and Reports (0704-0188), 1215 Jefferson Davis Highway, Suite 1204, Arlington, VA 22202-4302. Respondents should be aware that notwithstanding any other provision of law, no person shall be subject to any penalty for failing to comply with a collection of information if it does not display a currently valid OMB control number. PLEASE DO NOT RETURN YOUR FORM TO THE ABOVE ADDRESS.

1. REPORT DATE (DD-MM-YYYY) 13-01-1998		2. REPORT TYPE Paper		3. DATES COVERED (From - To)				
4. TITLE AND SUBTITLE Pentagonal Planar AX₅ Species: Synthesis and Characterization of the Iodine (III) Pentafluoride Dianion, IF₅						5a. CONTRACT NUMBER		
						5b. GRANT NUMBER		
						5c. PROGRAM ELEMENT NUMBER		
6. AUTHOR(S) Karl O. Christe ¹ ; William W. Wilson ¹ ; Greg W. Drake ² ; David A. Dixon; Jerry A. Boatz ² ; Robert Z. Gnann						5d. PROJECT NUMBER 2303		
						5e. TASK NUMBER M2C8		
						5f. WORK UNIT NUMBER		
7. PERFORMING ORGANIZATION NAME(S) AND ADDRESS(ES) AND ADDRESS(ES)						8. PERFORMING ORGANIZATION REPORT		
¹ Hughes STX Propulsion Directorate Air Force Research Laboratory Edwards AFB CA 93524		² Air Force Research Laboratory (AFMC) AFRL/PRS 5 Pollux Drive Edwards AFB CA 93524-7048						
9. SPONSORING / MONITORING AGENCY NAME(S) AND ADDRESS(ES) Air Force Research Laboratory (AFMC) AFRL/PRS 5 Pollux Drive Edwards AFB CA 93524-7048						10. SPONSOR/MONITOR'S ACRONYM(S)		
						11. SPONSOR/MONITOR'S NUMBER(S) AFRL-PR-ED-TP-1998-026		
12. DISTRIBUTION / AVAILABILITY STATEMENT Approved for public release; distribution unlimited.								
13. SUPPLEMENTARY NOTES								
14. ABSTRACT								
20020115 075								
15. SUBJECT TERMS								
16. SECURITY CLASSIFICATION OF:			17. LIMITATION OF ABSTRACT A	18. NUMBER OF PAGES	19a. NAME OF RESPONSIBLE PERSON Carl Ousley			
a. REPORT Unclassified					b. ABSTRACT Unclassified			c. THIS PAGE Unclassified
						19b. TELEPHONE NUMBER (include area code) (661) 275-6346		

Pentagonal Planar AX_5 Species: Synthesis and Characterization of the Iodine (III) Pentafluoride Dianion, $\text{IF}_5^{2-}\text{*}$

Karl O. Christe,^{*‡§} William W. Wilson,[†] Greg W. Drake,[#] David A. Dixon,^{||} Jerry A. Boatz,[#] and Robert Z. Gnann[§]

Hughes STX, Propulsion Directorate, Air Force Research Laboratory, Edwards Air Force Base, California 93524, Loker Hydrocarbon Research Institute, University of Southern California, Los Angeles, California 90089, and Pacific Northwest National Laboratory, Richland, Washington 99352.

Abstract: The new IF_5^{2-} dianion, which is only the second known example of a pentagonal planar AX_5 species, was prepared as its $\text{N}(\text{CH}_3)_4^+$ salt from $\text{N}(\text{CH}_3)_4\text{IF}_4$ and $\text{N}(\text{CH}_3)_4\text{F}$ in CH_3CN solution. Its structure was established by infrared and Raman spectroscopy, *ab initio* calculations and a comparison to isoelectronic XeF_5^- . Furthermore, vibrational spectroscopy and x-ray powder diffraction data show that the previously reported composition “ Cs_3IF_6 ” is actually a mixture of Cs_2IF_5 and CsF . Ab initio calculations also show that the most probable geometries for IF_6^{3-} are vibrationally unstable and undergo spontaneous F^- ion loss with formation of either pentagonal planar IF_5^{2-} or square planar IF_4^- . The synthesis and some properties of the new $\text{N}(\text{CH}_3)_4\text{IF}_4$ salt and a revised normal coordinate analysis of XeF_5^- are also presented.

Introduction

In 1991, the synthesis and characterization of the XeF_5^- anion was reported.¹ This anion is highly unusual as it is the only known example of a pentagonal planar AX_5 species. In our search for additional representatives of this class, it was noted that the Raman spectrum of a sample² having the analytical composition Cs_3IF_6 closely resembled that of CsXeF_5 . As the unknown IF_5^{2-} is isoelectronic with XeF_5^- and is likely to be isostructural, we suspected that the previously reported “ Cs_3IF_6 ” composition might actually be a mixture of CsF and Cs_2IF_5 . Fortunately, the original sample of “ Cs_3IF_6 ” had been preserved in our laboratory for 25 years and showed no signs of deterioration. Therefore, this sample was reinvestigated as it could possibly contain a pentagonal planar IF_5^{2-} dianion. Unfortunately, both CsF and the cesium salt of the multiply

charged anion present in the "Cs₃IF₆" sample were found to be insoluble in all available chemically inert solvents, thus preempting either their separation by extraction methods or the identification of the multiply charged anion by methods such as multinuclear NMR spectroscopy or growing of a single crystal for x-ray diffraction. It was therefore interesting to synthesize soluble IF₄⁻ and F⁻ salts containing a common cation, which would allow the determination of the true combining ratio of IF₄⁻ with F⁻. A comparison of the vibrational spectra of the resulting product with those of "Cs₃IF₆" should then also permit a positive identification of the anion present in "Cs₃IF₆".

Experimental

The original ²Cs₃IF₆ sample, prepared by the combination of CsF and IF₃ in a 3:1 mol ratio in a CFCl₃ suspension at -78°C,^{3,4} was used in this study. The preparation of IF₃,³ anhydrous N(CH₃)₄F⁵ and XeF₂⁶ have previously been described. The purity of the IF₃ was checked by its low temperature Raman spectrum which was in excellent agreement with a previous report.⁷ The N(CH₃)₄I (K & K Labortories, Inc.) was used as received. The CH₃CN (J.T. Baker, bioanalyzed, low water) was dried over P₂O₅ prior to its use. The volatile fluorine compounds were handled in a stainless-steel Teflon-FEP vacuum line, similar to one previously described.⁸ The CH₃CN was handled in a flamed out Pyrex glass vacuum line equipped with Kontes Teflon valves and a Heise pressure gauge.

Infrared spectra were recorded on a Perkin-Elmer Model 283 spectrophotometer using AgCl disks prepared by pressing the finely powdered sample between two thin AgCl plates in a Barnes Engineering minipress inside the glove box. An AgCl blank was placed into the reference beam to compensate for the absorption of the window material. Raman spectra were recorded on either a Cary Model 83GT, a Spex Model 1403 or a Bruker Equinox 55 spectrophotometer using the 488 nm exciting line of an Ar ion laser, the 647.1 nm line of a Kr ion laser or the 1064 nm line of a neodymium yag laser, respectively. ¹⁹F NMR spectra were recorded at 84.24 MHz on a Jeol FX902 multinuclear instrument between +30 and -30 °C, using CH₃CN as a solvent and d6-

acetone/CFCl₃ as an external lock substance and standard. The DSC data were recorded using a DuPont Model 910 DSC. A DuPont Model 2000 Thermal Analyst was used for recording and analyzing the data. The samples were crimp sealed in aluminum pans inside the drybox and heated at a rate of 2 °C/min.

Synthesis of N(CH₃)₄IF₄. Inside the dry box, N(CH₃)₄I (2.163 mmol) and XeF₂(4.327 mmol) were combined in a prepassivated (with ClF₃) Teflon FEP, 0.75 inch o.d. Teflon FEP U-tube which was closed with two stainless steel valves. On the glass vacuum line, CH₃CN (10 mL liquid) was added at -196 °C, and the mixture was warmed to -31 °C. After 8 hr, all gas evolution had ceased, and the amount of gas volatile at -78 °C (2.1 mmol of Xe) was measured. A white solid had formed in the bottom of the tube which was identified as N(CH₃)₄IF₂.⁹ Upon warming of the mixture to room temperature, the yellowish CH₃CN solution turned more orange and additional gas evolved. After 1.5 hr at 20 °C, the gas evolution (2.13 mmol of Xe) was complete, resulting in a white solid and clear orange-yellow solution. All volatile material was pumped off at room temperature leaving behind 602 mg of a white solid (weight calcd for 2.163 mmol of N(CH₃)₄IF₄ = 599.4 mg) which was identified by vibrational and NMR spectroscopy as N(CH₃)₄IF₄.

N(CH₃)₄IF₄ was also prepared by the reaction of stoichiometric amounts of N(CH₃)₄F and IF₃ in CH₃CN solution of -31 °C. However, this synthesis is inferior to the one described above.

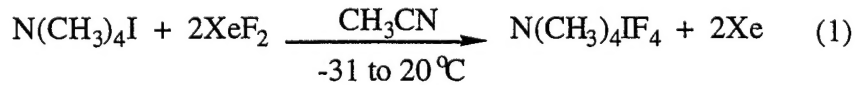
Synthesis of [N(CH₃)₄]₂IF₅. Inside the dry box, N(CH₃)₄IF₄ (0.58 mmol) and N(CH₃)₄F (0.72 mmol) were loaded into a prepassivated, 0.75 inch o.d., Teflon-FEP ampoule which contained a Teflon coated magnetic stirring bar and was closed by a stainless steel valve. On the glass line, dry CH₃CN (7.2 mL) was added at -196 °C and the mixture was stirred for 18 hr at -31 °C. The solvent was pumped off for 14 hr, first at -31 °C and during the last stages at room temperature, resulting in a white dry solid (227 mg, weight calcd for 0.58 mmol

$[N(CH_3)_4]_2IF_5$ plus 0.14 mmol $N(CH_3)_4F$ = 228 mg) which was shown by vibrational spectroscopy to consist mainly of $[N(CH_3)_4]_2IF_5$, containing a small amount of unreacted $N(CH_3)_4IF_4$ and the excess of $N(CH_3)_4F$ used in the reaction.

Theoretical Calculations. Electronic structure calculations were done at the local density functional theory (LDFT) level^{10,11} with a polarized valence double zeta basis set (DZVP)¹², and at the Hartree-Fock (HF) level¹³ with an effective core potential (ECP)¹⁴ on I for the core electrons and with a polarized double zeta basis set for the valence electrons, and with an all electron polarized double zeta valence set on F.¹⁵ Geometries were optimized using analytical methods.¹⁶ Analytic second derivatives were calculated at the optimized LDFT geometries.¹⁷ Numerical second derivatives were calculated at the Hartree-Fock level by using a two-point differencing scheme. The LDF calculations were done with DGauss¹⁸, and the HF calculations were done with Gaussian 94.¹⁹ The calculated Hessian matrices (second derivatives of the energy with respect to Cartesian coordinates) were converted to symmetry-adapted internal coordinates for further analysis using the program systems GAMESS²⁰ and Bmtrx.²¹

Results and Discussion

Synthesis and Properties of $N(CH_3)_4IF_4$. As already pointed out in the Introduction, the determination of the combining ratio of IF_4^- with F^- required the availability of soluble salts of these two anions with a common counterion. Since $N(CH_3)_4F^5$ and $N(CH_3)_4XF_4$ ($x = Br$ or Cl)²² were known to have good solubility in CH_3CN , the $N(CH_3)_4IF_4$ salt appeared to be an ideal candidate for our reactions. Our first attempts to prepare this salt from $N(CH_3)_4F$ and IF_3 in CH_3CN solution at -31 °C produced only impure products. Subsequently, the following improved synthesis (1) gave very pure $N(CH_3)_4IF_4$, eliminated the need for the thermally unstable IF_3 , which is difficult to purify,^{3,4} and utilized only commercially available starting materials. It is



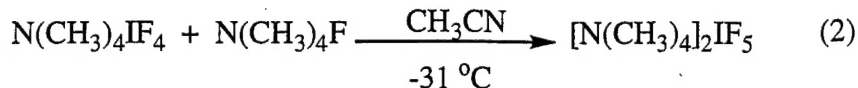
similar to the one previously reported²³ for 1,1,3,3,5,5 hexamethylpiperidinium (pip^+) IF_4^- from pip^+F^- , iodine and XeF_2 , but offers the advantages of avoiding a 7 step, 14% yield synthesis of pip^+F^- and the handling of volatile elemental iodine.

$\text{N}(\text{CH}_3)_4\text{IF}_4$ is a white crystallinic solid which, based on DSC data and vibrational spectra, undergoes a reversible endothermic phase change of 21.8 J/g at 73.8 °C and irreversible exothermic decomposition at 284 °C. The surprisingly high thermal stability of this compound is in marked contrast to that of $\text{pip}^+\text{IF}_4^-$ which was reported²³ to be unstable above 0 °C.

The ^{19}F NMR spectra of $\text{N}(\text{CH}_3)_4\text{IF}_4$ in CH_3CN solution were recorded at -30 and 30 °C and consisted of broad singlets at $\delta = -106.5$ with half widths of 385 and 1061 Hz, respectively. The observed chemical shift is in excellent agreement with the value of -106 ppm, previously reported²³ for $\text{pip}^+\text{IF}_4^-$ in CH_3CN at -20 °C. The chemical shift of IF_4^- fits nicely the trends observed for other halogen fluoride anions,^{25,26} i.e., the shielding of the fluorine ligands decreases with increasing oxidation state and electronegativity of the central atom (see Table 1). Pronounced line broadening with increasing temperature was also observed for BrF_4^- and ClF_4^- .²⁶

The infrared and Raman spectra of $\text{N}(\text{CH}_3)_4\text{IF}_4$ are summarized in Table 2. The bands observed for the IF_4^- part of $\text{N}(\text{CH}_3)_4\text{IF}_4$ agree well with those previously reported for CsIF_4 ,² but not with those (Ra: 573.5, 461 and 213 cm^{-1}) previously listed²³ for $\text{pip}^+\text{IF}_4^-$. Particularly, the value of 573.5 cm^{-1} , reported for $\nu_1(\text{A}_{1g})$ of $\text{pip}^+\text{IF}_4^-$, is outside the expected (see Computational Results below) range and is likely incorrect. The bands due to the $\text{N}(\text{CH}_3)_4^+$ cation have been summarized in a footnote of Table 2. They are in excellent agreement with those previously reported for other $\text{N}(\text{CH}_3)_4^+$ salts^{1,5,9} and, therefore, do not require further discussion.

Synthesis and Properties of $[\text{N}(\text{CH}_3)_4]_2\text{IF}_5$. The combination of $\text{N}(\text{CH}_3)_4\text{IF}_4$ with a slight excess of $\text{N}(\text{CH}_3)_4\text{F}$ in CH_3CN solution at -31 °C produced the desired $[\text{N}(\text{CH}_3)_4]_2\text{IF}_5$ (2).



Prolonged reaction times (about 20 hr) and stirring resulted in an almost quantitative conversion of IF_4^- to IF_5^{2-} thus establishing the 1:1 combining ratio between IF_4^- and F^- . In the presence of a large excess of F^- ions, no further fluoride ion uptake and, hence, no formation of IF_6^{3-} were observed. Attempts to carry out reaction (2) in CHF_3 solution at -78°C were unsuccessful and only unreacted $\text{N}(\text{CH}_3)_4\text{IF}_4$ was recovered.

The $[\text{N}(\text{CH}_3)_4]_2\text{IF}_5$ salt is a white solid which is stable at room temperature. It has very little solubility in solvents, such as CH_3CN , which precluded its characterization by NMR spectroscopy and the growing of single crystals for a crystal structure determination. Infrared and Raman spectra of the solid were used for its characterization. They are given in Figure 1 and Table 3, and their assignments are discussed below in more detail.

Characterization of Cs_2IF_5 . In the original report² on “ Cs_3IF_6 ”, the true combining ratio of IF_3^- with CsF had not been established. An arbitrary 1:3 ratio of the starting materials had been used and, since both, CsF and Cs_2IF_5 , are insoluble, the products could not be separated and, therefore, by necessity had the analytical composition Cs_3IF_6 .

In the reaction of IF_4^- with an excess of fluoride ions, the logical first step is the addition of one fluoride ion with formation of IF_5^{2-} . The addition of a second fluoride ion with formation of an IF_6^{3-} trianion becomes less likely since the Lewis acidity of the parent anion decreases with the addition of each F^- ion. Although, based on these arguments, the formation of IF_5^{2-} is clearly favored over that of IF_6^{3-} , it previously had not been given much consideration due to the absence of any other AX_5E_2 species containing two free valence electron pairs (E) on A. This picture, however, has changed recently with the synthesis of surprisingly stable XeF_5^- salts.¹

Our reinvestigation of the original² “ Cs_3IF_6 ” sample, which had been preserved in our laboratory for 25 years without noticeable decomposition, showed that it is indeed a mixture of Cs_2IF_5 and CsF , based on the following evidence:

- (i) X-ray powder data: The previously published powder pattern of "Cs₃IF₆" (Table II of reference 2) shows all the lines characteristic²⁷ for CsF ($d(\text{\AA})$, intens: 3.4 ms, 3.03 mw, 2.106 mw, 1.801 mw, 1.735 vw, 1.496 w, 1.370w, 1.336 mw, 1.223 w, 1.153w) and leaves no doubt that "Cs₃IF₆" contains a very significant amount of free CsF.
- (ii) Infrared spectrum: The infrared spectrum of "Cs₃IF₆" was rerecorded and compared to that of CsF taken under the same conditions. It was found that the major absorption in both spectra was a very intense and broad band at 298 cm⁻¹ due to CsF which in the "Cs₃IF₆" case confirms the presence of free CsF but obscures the less intense IF₅²⁻ bands.
- (iii) Raman spectrum: A higher quality Raman spectrum, which did not suffer from fluorescence,² was obtained by means of 1064 nm excitation with a neodymium yag laser and is shown in Figure 2. The dominant Raman bands at 478, 396, 339 and 325 cm⁻¹ are in excellent agreement with those of IF₅²⁻ in [N(CH₃)₄]₂IF₅ (see Table 3) and leave no doubt that the dominant anion in "Cs₃IF₆" is IF₅²⁻. For a hypothetical IF₆³⁻ anion, the additional fluoride ligand and extra formal negative charge should cause a different band pattern and significant shifts to lower frequencies. In addition to the intense IF₅²⁻ bands, the "Cs₃IF₆" spectrum showed several very weak bands which can be assigned to likely impurities, such as IF₇²⁻ (556 and 454 cm⁻¹) or IOF₅²⁻ (865 cm⁻¹)²⁸ and lattice vibrations (140 and 110 cm⁻¹). The formation of IF₇²⁻ and IOF₅²⁻ can be easily rationalized. Iodine trifluoride has a tendency to disproportionate to I₂ and IF₅,³ and IF₅ is known²⁸ to react with excess F⁻ to give IF₇²⁻. Similarly, a trace of moisture will result in partial hydrolysis of IF₆⁻ to give IOF₄⁻, which in turn is known to give with excess F⁻ the IOF₅²⁻ dianion.²⁸ These impurities had been formed already during the original preparation⁴ and were not generated during sample storage.

Vibrational Spectra and Electronic Structure Calculations. The vibrational spectra of IF₅²⁻ are summarized in Table 3 and were assigned by analogy with those established for the isoelectronic XeF₅⁻ anion.^{1,29} The only difference is the reversal of the identity of v₅ and v₆ in the E₂ block, based on the results of the potential energy distribution (see below). The spectra of IF₅²⁻ and

XeF_5^- are very similar. They exhibit the expected frequency decreases for IF_5^{2-} due to the additional negative charge which enhances the $\text{X}(\delta+)-\text{F}(\delta-)$ polarity of the bonds. Analogous general frequency and bond weakening effects are also observed on going from IF_4^- (see Table 2) to IF_5^{2-} (see Table 3).

The geometry and the vibrational spectra of IF_5^{2-} and XeF_5^- were studied by electronic structure calculations at the HF and LDFT levels. To evaluate the reliability of our computational methods, the well known IF_4^- geometry²³ and spectra² were calculated first. As can be seen from Tables 2 and 4, the HF/ECP/DZP method gave the better results. For IF_4^- , the bond length, calculated at the HF/EDP/DZP level is only 0.013 Å shorter than the observed one.²³ For IF_5^{2-} , the minimum energy structure at both the HF and LDFT levels was pentagonal planar with D_{5h} symmetry. Assuming a similar correction as for IF_4^- , the bond length of IF_5^{2-} is predicted to be 2.11 Å. This bond length increase of 0.09 Å relative to IF_4^- can be explained by the increased polarity of the bonds (see above) and increased ligand-ligand repulsion due to a decrease of the F-I-F bond angle from 90 ° in IF_4^- to 72 ° in IF_5^{2-} .

The symmetry force constants and potential energy distributions (PED) were calculated for IF_5^{2-} and XeF_5^- using the scaled HF/ECP/DZP frequencies (see Table 5). Since we were unable to duplicate with our computer calculations the previously published, hand calculated, out of plane deformation force constants,^{1,29} the originally given¹ G matrix was reexamined and found to contain incorrect multiplicity factors for G_{22} and G_{77} . The corrected G matrix for XeF_5^- is given in Table 6 and was verified by the machine methods. A typographical error for a sign in one of the originally published¹ symmetry coordinates, i.e., (S_{5b}) should read $(2/5)^{1/2} [\sin 2\alpha(\Delta r_2 - \Delta r_5) - \sin \alpha(\Delta r_3 - \Delta r_4)]$ has already been corrected elsewhere.²⁹ The revised force constant, $F_{22} = 0.480$ mdyn Å/rad², for the symmetric out of plane deformation of XeF_5^- is now in much better agreement with our expectation. The deformations out of the highly crowded pentagonal plane should possess significantly smaller force constants than the corresponding in plane deformations.

As can be seen from Tables 3 and 5, the results from the normal coordinate analyses confirm the identities of these pentagonal planar anions. The general fit between the calculated and observed frequencies is very good. The only remaining minor ambiguities in the normal coordinate analyses are: (i) for XeF_5^- , the exact location of the infrared active, in plane deformation mode, v_4 , is somewhat uncertain. Based on the calculations, its frequency is similar to, but its infrared intensity is much lower than those of the out of plane umbrella deformation mode, v_2 . Therefore, we assume that v_4 is hidden under the v_2 band; (ii) for IF_5^{2-} , the location of the infrared active, out of plane umbrella deformation mode was obscured. In the Cs_2IF_5 spectrum, the strong absorption due to free CsF obscured this region, and in the $[\text{N}(\text{CH}_3)_4]_2\text{IF}_5$ spectrum, the presence of an IF_4^- impurity and the broadness of the v_3 mode of IF_5^{2-} interferred. In the Raman spectrum of Cs_2IF_5 , one of the two E_2' bands exhibits a splitting, similar to those observed for these modes in XeF_5^- . In Table 3, this splitting was tentatively assigned to v_5 because this requires a smaller splitting. However, if one assumes v_6 to be split instead of v_5 , the average of the 396 and 339 cm^{-1} components would result in much better agreement with the calculated frequency of 366 cm^{-1} and the $[\text{N}(\text{CH}_3)_4]_2\text{IF}_5$ spectrum, in which v_6 of IF_5^{2-} probably coincides with a cation band at 366 cm^{-1} .

An inspection of the potential energy distributions for IF_5^{2-} and XeF_5^- (see Table 5) shows that the E modes of XeF_5^- are considerably more characteristic than those of IF_5^{2-} . This is due to the increased bond polarity in IF_5^{2-} , which lowers preferably the stretching force constant and makes its value more similar to those of the deformation constants. This enhances the mixing of the normal modes in IF_5^{2-} and, in its E_2' block, results in the higher frequency mode becoming mainly the bending motion. A further consequence of the larger bond polarity in IF_5^{2-} is the increased coupling of the stretching motions involving opposite bonds ($f_{rr'} = 0.42 \text{ mdyn / } \text{\AA}$). This large $f_{rr'}$ value is responsible for the low frequency of the antisymmetric stretching mode, $v_3(E_1')$, which respresents

the reaction coordinate for the loss of an F⁻ ion. This finding is in accord with the observation that IF₅²⁻ readily loses an F⁻ ion to give IF₄⁻.

The stability of the hypothetical IF₆³⁻ anion was also examined by ab initio methods. The four most likely geometries of IF₆³⁻ are shown in Figure 3. Like IF₅²⁻, this anion contains two free valence electron pairs on iodine. If both electron pairs are sterically active, the most likely structure is the one with D_{3d} symmetry, in which the two more repulsive free pairs avoid each other as much as possible by occupying the axial trans positions of a bicapped octahedron. If, on the other hand, one of the two free valence electron pairs on iodine is sterically inactive, i.e., occupies an A_{1g} or s-orbital, only p and d-orbitals of iodine are involved in the bonding and, therefore, the resulting structures are governed by repulsion effects, and, as in transition metal heptafluorides,³⁰ the energetically most favored structures become the monocapped octahedron of C_{3v} symmetry and the monocapped trigonal prism of C_{2v} symmetry. The pentagonal bipyramidal of C_{5v} symmetry is slightly higher in energy, but was also considered.³¹⁻³³

The structures of all four geometries of IF₆³⁻ were calculated at the restricted Hartree-Fock (RHF) self-consistent field level, using effective core potentials³⁴ and the corresponding valence basis sets of Stevens, Basch, Krauss, and Jasien.³⁵ The basis set was augmented with a diffuse s+p shell³⁶ and a d polarization function³⁷ on each atom. All calculations were performed using the GAMESS quantum chemistry package.²⁰ Since the HOMO of the D_{3d} and C_{3v} structures is a half-filled degenerate orbital pair, Jahn-Teller distortion to lower symmetry is anticipated. Therefore, the initial geometries of these conformations were distorted to C_s symmetry by slight elongation of one pair of trans fluorine ligands. For each of the four conformations, geometry optimization led to the dissociative loss of one or two fluoride ligands. Specifically, optimization of the C_{2v} conformation and the distorted D_{3d} and C_{3v} structures led to formation of square planar [IF₄]⁻ and 2 fluoride anions, whereas optimization of the C_{5v} structure led to formation of pentagonal planar [IF₅]²⁻ and one fluoride anion. Thus, none of the four conformations were found to be a local minimum. Although more extensive calculations are desirable to definitively rule out the stability of the [IF₆]³⁻, the present results strongly indicate that this anion is not a stable species.

Conclusions

The successful synthesis of a second example of a pentagonal planar AX_5 species demonstrates that XeF_5^- is not a unique case, and that other examples of AX_5 molecules of D_{5h} symmetry, such as TeF_5^{3-} , AuF_5^{2-} or PtF_5^{3-} , might also exist. Although IF_5^{2-} had been prepared 30 years ago,³ its nature had not been recognized until now. The greatly delayed recognition of this unusual anion parallels the discovery¹ of XeF_5^- which had originally been mistaken for octahedral XeF_6^{2-} .³⁸⁻⁴⁰

Acknowledgments

The authors thank Drs. M. Petrie, K. Chaffee, P. Jones, and N. Kawai for their help with the NMR, x-ray diffraction, DSC, and Raman data, respectively, and Dr. S. Rogers and Prof. G. Olah for their active support. The work at the Air Force Research Laboratory was financially supported by the Propulsion Directorate and Office of Scientific Research of the U.S. Air Force, that at USC by the National Science Foundation, and that at PNNL by the U.S. Department of Energy. Scholarships from the Deutsche Forschungsgemeinshaft (R.Z.G.) and the National Research Council (G.W. D.) are greatfully acknowledged.

References

- ♥ Dedicated to Professor Neil Bartlett on the occasion of his 65th birthday
- ‡ Hughes STX
- § University of Southern California
- || Pacific Northwest National Laboratory
- # Propulsion Directorate, Air Force Research Laboratory
- (1) Christe, K.O.; Curtis, E.C.; Dixon, D.A.; Mercier, H.P.; Sanders, J.C.P.; Schrobilgen, G.J. *J. Am. Chem. Soc.* **1991**, *113*, 3351.
- (2) Christe, K.O.; Naumann, D. *Inorg. Chem.* **1973**, *12*, 59.
- (3) Schmeisser, M.; Ludovici, W.; Naumann, D.; Sartori, P.; Scharf, E. *Chem. Ber.* **1968**, *101*, 4214.
- (4) Schmeisser, M.; Sartori, P.; Naumann, D. *Chem. Ber.* **1970**, *103*, 590.
- (5) Christe, K.O.; Wilson, W.W.; Wilson, R.D.; Bau, R.; Feng, J. *J. Am. Chem. Soc.* **1990**, *112*, 7619, and references cited therein.
- (6) Frlec, B.; Holloway, J.H. *J.C.S. Dalton* **1975**, 535.
- (7) Schmeisser, M.; Naumann, D.; Lehmann, E. *J. Fluorine Chem.* **1973/74**, *3*, 441.
- (8) Christe, K.O.; Wilson, R.D.; Schack, C.J. *Inorg. Synth.* **1986**, *24*, 5.
- (9) Christe, K.O.; Wilson, W.W.; Drake, G.W.; Petrie, M.A.; Boatz, J.A. *J. Fluorine Chem.* in press.
- (10) (a) Parr, R.G.; Yang, W. *Density Functional Theory of Atoms and Molecules*. Oxford University Press, New York, **1989**; (b) Labanowski, J.; Andzelm, J.,Eds. *Density Functional Methods in Chemistry*. Springer Verlag, New York, **1991**; (c) Ziegler, T. *Chem. Rev.* **1991**, *91*, 651; (d) Salahub, D.R. in *Ab Initio Methods in Quantum Chemistry-II*, K.P. Lawley, Ed. J. Wiley & Sons, New York. p. 447, **1987**; (e) Jones, R.O.; Gunnarsson, O. *Rev. Mod. Phys.* **1989**, *61*, 689.
- (11) Vosko, S.J.; Wilk, L.; Nusair, W. *Can. J. Phys.* **1980**, *58*, 1200.

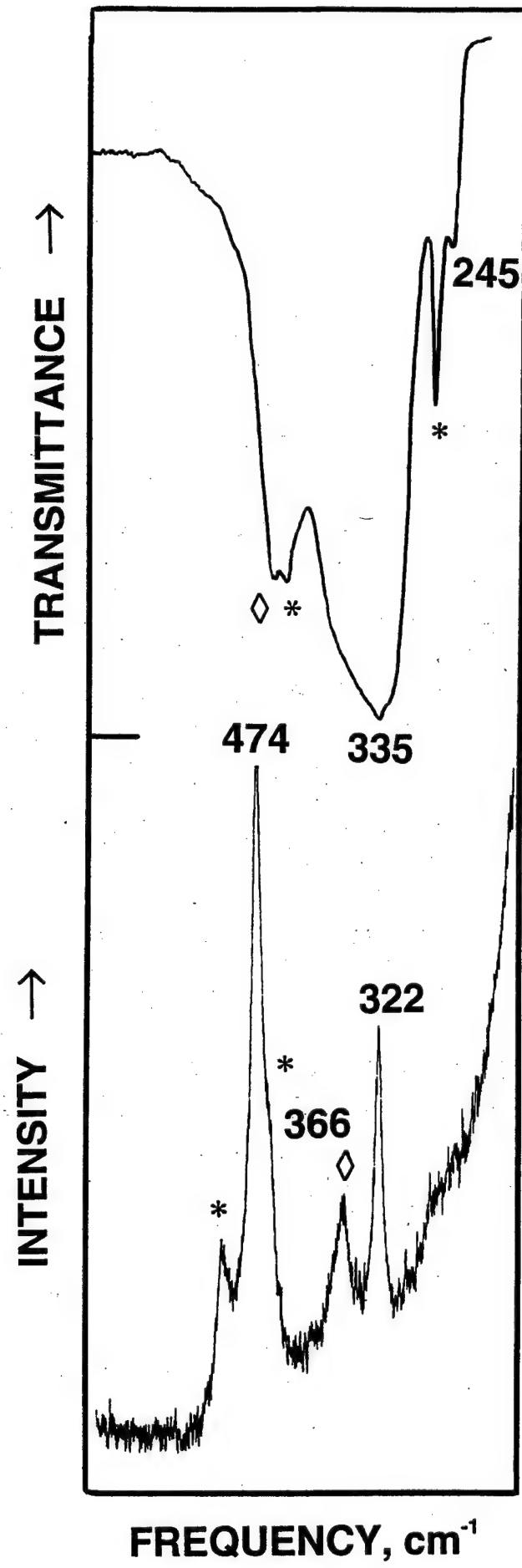
- (12) Godbout, N; Salahub, D.R.; Andzelm, J.; Wimmer, E. *Can. J. Chem.* **1992**, *70*, 560.
- (13) (a) Hirst, D.M. "A Computational Approach to Chemistry" *Blackwell Scientific*, Oxford (1990); (b) Grant, G.H.; Richards, W.G. "Computation Chemistry" Oxford University Press, Oxford (1995); (c) Hehre, W.J.; Radom, L.; Schleyer, P.v.R.; Pople, J.A. "Ab Initio Molecular Orbital Theory" John Wiley and Sons, New York (1986).
- (14) Hay, P.J.; Wadt, W.R. *J. Chem. Phys.*, **82**, 270, 284, 299 (1985).
- (15) Dunning, T.H., Jr.; Hay, P.J. in "Methods of Electronic Structure Theory," Schaefer, H.F., III; Plenum Press: New York, **1977**, Ch. 1.
- (16) (a) Komornicki, A.; Ishida, K.; Morokuma, K.; Ditchfield, R.; Conrad, M. *Chem. Phys. Lett.* **1977** *45*, 595. (b) McIver, J.W., Jr.; Komornicki, A. *Chem. Phys. Lett.* **1971**, *10*, 202. (c) Pulay, P. in "Applications of Electronic Structure Theory," Schaefer, H.F. III, Ed.; Plenum Press: New York, **1977**, p.153.
- (17) Komornicki, A.; Fitzgerald, G. *J. Phys. Chem.* **1993**, *98*, 1398 and references therein.
- (18) (a) Andzelm, J.; Wimmer, E.; Salahub, D.R. in *The Challenge of d and f Electrons: Theory and Computation*; Salahub, D.R.; Zerner, M.C., Eds; ACS Symposium Series, No 394, American Chemical Society: Washington D.C., 1989; p.228. (b) Andzelm, J. in "Density Functional Theory in Chemistry;" Labanowski, J.; Andzelm, J., Eds.; Springer-Verlag: New York, 1991, p. 155. (c) Andzelm, J.W.; E. *J. Chem. Phys.* **1992**, *96*, 1280.
- (19) *Gaussian 94*, Frisch, M.J.; Trucks, G.W.; Schlegel, H.B.; Gill, P.M.W.; Johnson, B.G.; Robb, M.A.; Cheeseman, J.R.; Keith, T.A.; Peterson, G.A.; Montgomery, J.A.; Raghavachari, K.; Al-Laham, M.A.; Zakrzewski, V.G.; Ortiz, J.V.; Foresman, J.B.; Cioslowski, J.; Stefanov, B.B.; Nanayakkara, A.; Challacombe, M.; Peng, C.Y.; Ayala, P.Y.; Chen, W.; Wong, M.W.; Andres, J.L.; Replogle, E.S.; Gomperts, R.; Martin, R.L.; Fox, D.J.; Binkley, J.S.; Defrees, D.J.; Baker, J.; Stewart, J.J.P.; Head-Gordon, M.; Gonzalez, C.; and Pople, J.A., Gaussian, Inc., Pittsburgh, PA, 1995.

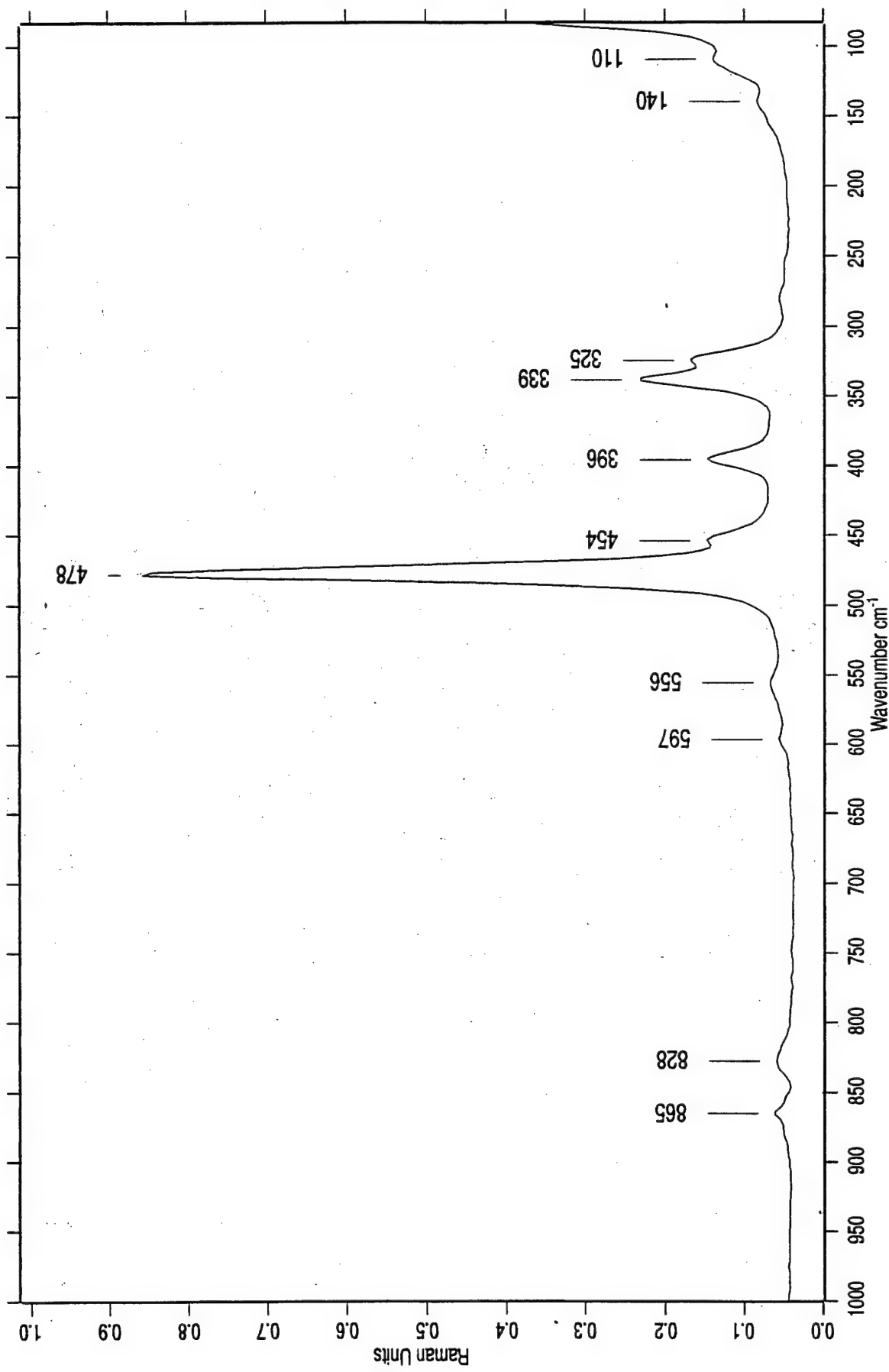
- (20) Schmidt, M.W.; Baldridge, K.K.; Boatz, J.A.; Elbert, S.T.; Gordon, M.S.; Jensen, J.H.; Koseki, S.; Matsunaga, N.; Nguyen, K.A.; Su, S.J.; Windus, T.L.; Dupuis, M.; Montgomery, J.A. *J. Comput. Chem.* **1993**, *14*, 1347.
- (21) Bmtrx version 2.0 Komornicki, A.; Polyatomics Research Institute: Palo Alto, CA, 1996.
- (22) Wilson, W.W.; Christe, K.O. *Inorg. Chem.* **1989**, *28*, 4172.
- (23) Zhang, X.; Seppelt, K. *Z. Anorg. Allg. Chem.* **1997**, *623*, 491.
- (24) Mahjoub, A.R.; Zhang, X.; Seppelt, K. *Chem. Europ. J.* **1995**, *1*, 261.
- (25) Christe, K.O.; Wilson, W.W. *Inorg. Chem.* **1989**, *28*, 3275.
- (26) Christe, K.O.; Sanders, J.C.P.; Schrobilgen, G.J.; Wilson, W.W. *J.C.S. Chem. Commun.* **1991**, 837.
- (27) National Bureau of Standards (U.S.) Mono. **25** Sect. 3 (1964).
- (28) Christe, K.O.; Wilson, W.W.; Drake, G.W. unpublished results.
- (29) Christe, K.O.; Dixon, D.A.; Mahjoub, A.R.; Mercier, H.P.A.; Sanders, J.C.P.; Seppelt, K.; Schrobilgen, G.J.; Wilson, W.W. *J. Am. Chem. Soc.* **1993**, *115*, 2696.
- (30) Giese, S.; Seppelt, K. *Angew. Chem. Int. Ed. Engl.* **1994**, *33*, 461.
- (31) Kepert, R.J. *Inorganic Stereochemistry*; Springer: Berlin, 1982.
- (32) Hoffmann, R.; Beier, B.F.; Muettterties, E.L.; Rossi, A.R. *Inorg. Chem.* **1977**, *16*, 511.
- (33) Gillespie, R.J.; Hargittai, I. *The VSEPR Model of Molecular Geometry*; Allyn and Bacon, A Division of Simon & Schuster, Inc.: Needham Heights, MA, 1991.
- (34) a) Melius, C.F.; Goddard, W.A. *Phys. Rev.A.* **1974**, *10*, 1528.
b) Kahn, L.R.; Baybutt, P.; Truhlar, D.G. *J. Chem. Phys.* **1976**, *65*, 3826.
c) Krauss, M.; Stevens, W.J. *Ann. Rev. Phys. Chem.* **1985**, *35*, 357.
- (35) a) Stevens, W.J.; Basch, H.; Krauss, M. *J. Chem. Phys.* **1984**, *81*, 6026.
b) Stevens, W.J.; Basch, H.; Krauss, M.; Jasien, P. *Can. J. Chem.* **1992**, *70*, 612.
- (36) The exponents of the diffuse s+p shells for iodine and fluorine are 0.0368 and 0.1076, respectively.
- (37) The d function exponents for iodine and fluorine are 0.266 and 0.8, respectively.

- (38) Spitzin, V.I.; Kiselev, Yu. M.; Fadeeva, N.E.; Popov, A.I.; Tchumaevsky, N.A. Z. *Anorg. Allg. Chem.* **1988**, 559, 171.
- (39) Kiselev, Yu.M.; Goryachenkov, S.A.; Martynenko, L.I.; Spitsyn, V.I. *Dokl. Akad. Nauk SSSR* **1984**, 278, 881.
- (40) Kiselev, Yu.M.; Fadeeva, N.E.; Popov, A.I.; Korobov, M.V.; Nikulin, V.V.; Spitsyn, V.I. *Dokl. Akad. Nauk SSSR* **1987**, 295, 378.

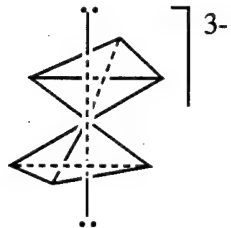
Diagram Captions

- Figure 1 Infrared and Raman spectra of solid $[N(CH_3)_4]_2 IF_5$. The bands masked by asterisks and diamonds are due to IF_4^- and $N(CH_3)_4^+$, respectively, while those marked by frequency values belong to IF_5^{2-} .
- Figure 2 Raman spectrum of Cs_2IF_5 .
- Figure 3 Most likely geometries of the IF_6^{3-} trianion and their spontaneous decomposition modes.

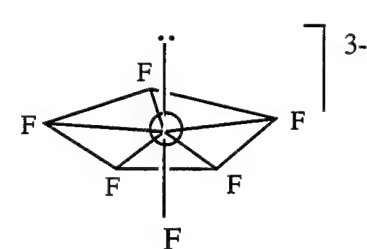
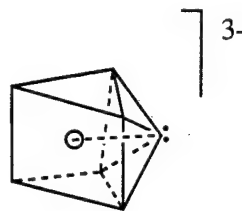
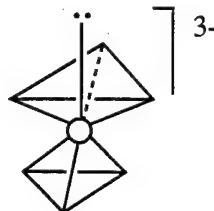




Two sterically active free valence electron pairs



One sterically active and one sterically inactive free valence electron pair



D_{3d}
BICAPPED
OCTAHEDRON

C_{3v}
MONOCAPPED
OCTAHEDRON

C_{2v}
MONOCAPPED
TRIGONAL PRISM

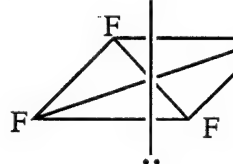
C_{5v}
PENTAGONAL
BIPYRAMID

$-2F^-$

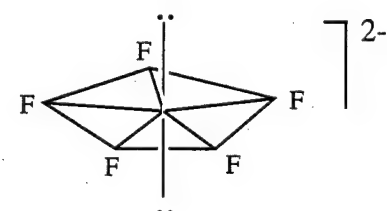
$-2F^-$

$-2F^-$

$-F^-$



D_{4h}
SQUARE
PLANAR



D_{5h}
PENTAGONAL
PLANAR

Table 1. ^{19}F Chemical Shifts for Binary Halogen Fluoride Anions

oxidation state of central atom	
+I	IF_2^- -282 ^a
+III	IF_4^- -106 ^b
+V	IF_6^- 13 ^c
+VII	IF_8^- 249 ^d

^a, ref 9. ^b this work and ref 23. ^c ref 25. ^d ref 26. ^e ref 22.



Table 2. Observed and Calculated Vibrational Spectra of IF_4^-

assigns and approx mode descriptions in point group D_{4h}			obsd freq, cm^{-1} (rel int) ^a			calcd freq, cm^{-1} (IR int) ^b		
Ra	A_{1g}	ν_1 ν sym in phase	IR	CsIF_4 IR	$\text{N(CH}_3)_4\text{IF}_4^d$ RA	HF/ECP/DZP unscaled	LDFT/DZVP unscaled	LDFT/DZVP scaled
IR	A_{2u}	ν_2 δ umbrella	271ms	—	522(10)	—	515(10)	559(0)
Ra	B_{1g}	ν_3 ν sym out of phase	—	—	455(7.2)	—	457(5.6)	493(0)
Ra	B_{2g}	ν_4 δ scissor	—	—	195(0+)	—	197(0.5)	225(0)
—	B_{2u}	ν_5 δ pucker	—	—	—	—	185(0)	157
IR	E_u	ν_6 ν asym	448vs	—	449 vs	—	481(951)	447
		ν_7 δ asym	n. obsd	—	n. obsd	—	139(3)	118
								115(3)

^aData for CsIF_4 from ref 2, for $\text{N(CH}_3)_4\text{IF}_4^-$ from this study. ^bInfrared intensities in km/mol. Empirical scaling factors of 0.9294 and 0.8490 for the stretching and deformation modes, respectively, were used to maximize the fit between the observed and calculated frequencies. ^dIn addition to the above listed IF^- bands, the following bands due to $\text{N(CH}_3)_4^+$ were observed: IR: 3118sh, 3040w, 2969vv, 1490 mw, 1444w, 1416mw, 1287w, 952m, 922w, 462m; Ra: 3021(0.7), 2969(0.2), 2942(0.4), 2907(0.1), 2800(0.1), 1471(0.6), 1461(0.7), 1413(0.3), 1284(0.1), 1175(0.15), 1168(0.1), 947(1.5), 754(1.5), 450 sh on the intense 457 IF_4^- band, 369(0.2).

Table 3. Observed and Calculated Vibrational Spectra of IF_5^{2-} Compared to Those Observed for XeF_5^-

			IF_5^{2-}			XeF_5^-		
assgnts and approx mode descriptions in point group D_{3h}			obsd freq, cm^{-1} (rel int) Cs_2IF_5 RA			calcd freq, cm^{-1} (IR int) HF/ECP/DZP scaled ^a		
Ra	A_1'	ν_1 sym	478(10)	474(10)	487(0)	468	504(10)	502(10)
IR	A_2''	ν_2 δ umbrella	(-) ^c		320(97)	307	274s	278s
IR	E_1'	ν_3 ν asym	335vs,br		356(588)	342	450vs 415s	509sh 465vs 420sh
					259(14)	249	288sh	
Ra	E_2'	ν_4 δ asym in plane	245w		322(3.8)	349(0)	432(1.5)	423(2.1)
					325(1.6)		422(1.6)	
Ra		ν_5 ν asym	339(2)		(366) ^d	381(0)	380(2.2) 369(2.3)	377(3.3)
						104(0)	100	
Ra	E_2''	ν_7 δ pucker						

^aData from ref 1. ^b In addition to the above listed IF_5^{2-} bands, the following bands due to $\text{N}(\text{CH}_3)_4^+$ were observed: IR: 3034ms, 1507ms, 1415w, 1255m, 963s, 467m; Ra: 3010(1.3), 2943(0.8), 2810(0.4), 1478(1.8), 952(1.8), 751(3.0), 460(sh), 366(1.0). ^cThis band is masked by the very intense broad band at 335 cm^{-1} . ^dThis band is obscured by the relatively intense 366 cm^{-1} $\text{N}(\text{CH}_3)_4^+$ band. ^eAn empirical scaling factor of 0.9606 was used to maximize the fit between observed and calculated frequencies. Ir intensities in km/mol.

Table 4. Calculated, Observed and Predicted Bond Lengths for IF_4^- and IF_5^{2-}

	bond distances (\AA)			predicted	
	observed	calculated	HF/ECP/DZP	LDFT/DZVP	
$\text{IF}_4^-(\text{D}_{4h})$	2.007 ^a	1.994	2.069	—	
$\text{IF}_5^{2-}(\text{D}_{5h})$	—	2.094	2.163	2.11	

^a Ref. 23.

Table 5. Symmetry Force Constants and Potential Energy Distribution of D_{3h} , IF_5^{2-a} and XeF_5 Calculated from the Scaled HF/ECP/DZP Second Derivatives

		IF_5^{2-a}		XeF_5^{2-b}		
freq, cm ⁻¹		sym force consts ^c	PED (%)	freq, cm ⁻¹	sym force consts ^c	
obsd	calcd	obsd	calcd	obsd	calcd	
A_1'	474	468	$F_{11} = 2.445$	100(1)	502	503
A_2''		307	$F_{22} = 0.529$	100(2)	278	305
E_1'	335	342	$F_{33} = 0.867$	70(3),20(4)	455	454
E_2'	245 322/339	249 335	$F_{34} = -0.030$ $F_{44} = 1.886$ $F_{55} = 1.735$	80(4),20(3) 74(5),26(6)	278 423	276 425
E_2''	366/396	366 100	$F_{56} = 0.115$ $F_{66} = 1.316$ $F_{77} = 0.260$	74(6),26(5) 100(7)	377 107	378 107

internal force constants

fr	1.529	2.043
frr	0.035	0.137
frr'	0.423	0.260

^aEmpirical scaling factors of 0.9606 and (0.9606)² were used for the frequencies and force constants, respectively. ^bScaling factors: 0.87322 and (0.87322)². ^cStretching constants in mdyn Å/rad², and stretch-bend interaction constants in mdyn/rad.

Table 6. G Matrix^a for Pentagonal Planar XeF₄⁻ of Symmetry D_{5h}

A ₁ '	G ₁₁ = μ _y = 5.2637 x 10 ⁻²
A ₂ "	G ₂₂ = (5/r ²)(μ _y + 5μ _x) = 1.1201 x 10 ⁻¹
E ₁ '	G ₃₃ = μ _y + 5μ _x /2 = 7.1679 x 10 ⁻²
	G ₃₄ = (5 ^{3/2} μ _x)/(4rsinα) = 1.1123 x 10 ⁻²
	G ₄₄ = (1/r ²)(5μ _y sin ² 2α + μ _x) = 2.4334 x 10 ⁻²
E ₂ '	G ₅₅ = μ _y = 5.2637 x 10 ⁻²
	G ₅₆ = 0
	G ₆₆ = (1/r ²)(4μ _y sin ² α) = 4.7026 x 10 ⁻²
E ₂ "	G ₇₇ = (3-5 ^{1/2})(5/2r ²)μ _y = 2.4823 x 10 ⁻²

^aThe following geometry and masses were used for the calculation of the G matrix:
 r = 2.0124 Å and α = 72°; m_x = 131.292; m_y = 18.998.